Comparison of the Impact of the 1982/83 and 1986/87 Pacific SST Anomalies on Time-Mean Predictions of Atmospheric Circulation

M. J. FENNESSY AND J. SHUKLA

Center for Ocean–Land–Atmosphere Interactions, University of Maryland, College Park, Maryland

(Manuscript received 24 August 1989, in final form 6 December 1990)

ABSTRACT

The primary focus of this study is to contrast the impact of the El Niño Pacific sea surface temperature (SST) anomalies observed during the Northern Hemisphere winters of 1982/83 and 1986/87 on predictions with a global general circulation model (GCM). The former event was an El Niño of record magnitude while the latter was of more typical magnitude. For each year, three 60-day control integrations with climatological boundary conditions and three 60-day boundary integrations with the observed SST only in the Pacific were performed with the Goddard Laboratory for Atmospheric Sciences GCM.

Among the observed tropical features correctly simulated in both cases are the large positive precipitation anomalies in the Pacific, the Southern Oscillation signal in the sea-level pressure field, and the upper-level easterly wind anomalies. However, the overall simulation of the observed tropical circulation anomalies is considerably better in 1982/83 than in 1987. Some extratropical features are also well simulated, although neither their accuracy nor the differences between the two years are as clear as in the tropics. An analysis of the SST impact on model forecast skill reveals that the impact is mainly on 60-day time means, rather than shorter means.

The results of an analysis of the anomalous divergence and effective Rossby wave source in the tropical and subtropical Pacific during these two years suggest that the primary observed and simulated extratropical circulation features may have been forced from the subtropics rather than the tropics. However, the relatively small magnitudes of the SST and precipitation anomalies in the subtropics make it likely that these subtropical divergence and Rossby wave source anomalies were themselves forced from the tropics.

1. Introduction

A wide variety of El Niño sea surface temperature (SST) anomaly studies has been performed by several modeling groups in recent years (for a brief review see Fennessy and Shukla 1988). Many of these studies were sensitivity experiments, utilizing simulations initialized from a climatological or random mean atmospheric state. A number of studies were carried out in order to determine the impact of observed Pacific SST anomalies on a model prediction initialized from, and compared to, the observed atmospheric state (WMO 1986; Owen and Palmer 1987; Tokioka et al. 1987; Shukla and Fennessy 1988).

Shukla and Fennessy (1988, hereafter SF) used the Goddard Laboratory for Atmospheric Sciences (GLAS) General Circulation Model (GCM) to examine the effect on prediction of the record El Niño SST anomalies of December, January, and February of 1982/83. They concluded that the 1982/83 Pacific SST anomalies had a very large impact on tropical prediction and a modest impact on extratropical prediction. The current study examines the impact on prediction with this same GCM of the 1986/87 Pacific SST anomalies, which were much more typical in magnitude than those in 1982/83. Results are compared to elucidate the differences in forecast impact from observed Pacific SST anomalies in these two very different El Niño years. The results are also examined to determine what time scales for prediction are impacted by the inclusion of the observed SST in an El Niño year.

In the tropics the SST impact on prediction is directly related to the altered heating patterns induced by the anomalous SST, and thus the difference between the tropical prediction impact in 1982/83 versus 1986/87 should be large and relatively straightforward. Understanding the impact on extratropical prediction in these two years is much more difficult. The horizontal pattern and equivalent barotropic structure of the extratropical circulation anomalies in these two years are reminiscent of Rossby wave dispersion on a sphere. Recent studies by Held and Kang (1987) and Sardeshmukh and Hoskins (1988) have pointed out the importance of anomalous divergence in the subtropics in forcing the extratropical flow. Held and Kang (1987) show that the extratropical wave train found in the response of a

Corresponding author address: Mr. Michael J. Fennessy, Center for Ocean–Land–Atmosphere Interactions, 2213 Computer and Space Science Building, University of Maryland, College Park, MD 20742-2425.

Geophysical Fluid Dynamics Laboratory (GFDL) GCM to El Niño SST anomalies was primarily forced from the anomalous convergence in the central subtropical Pacific. Sardeshmukh and Hoskins (1988) noted the importance of considering the full effective Rossby wave source rather than just the divergence when considering tropical or subtropical forcing. The lack of a clear relation between tropical SST anomalies and the forced extratropical response found in the current study as well as others (e.g., Geisler et al. 1985) is consistent with the hypothesis that the dominant extratropical forcing is not necessarily directly from the tropics. It may be that the tropical anomalies force subtropical anomalies which then force the extratropics. An attempt is made here to relate the anomalous divergence and effective Rossby wave source fields in the tropical and subtropical Pacific to the extratropical anomalies in both the observations and simulations for these two years.

2. Model and experiments

The GLAS GCM used here is global in extent with a 4° lat × 5° long grid and nine equally spaced sigma levels in the vertical. The planetary boundary layer is that of Deardorff (1972) as modified by Randall (1976). Supersaturation clouds occur at all nine levels, while convective clouds (Arakawa 1969) are limited to the lowest six levels. Further details of the model are given by Fennessy et al. (1985). The model winter climatology and climate drift are discussed by SF.

For each experiment year three 60-day control simulations with monthly varying climatological boundary conditions everywhere and three 60-day boundary simulations with identical boundary conditions everywhere except the Pacific were done. The SST climatology used is based on a GFDL analysis of SST data published by the United States Navy (1964). For the boundary simulations the observed monthly SST anomalies obtained from the Climate Analysis Center (CAC) were added to the monthly climatological values used in the control simulations for the region of the Pacific from 40°S to 60°N for 1982/83 and from 60°S to 60°N for 1987. The model linearly interpolates to daily values during integration. National Meteorological Center (NMC) observed atmospheric conditions for 0000 UTC 15, 16, 17 December 1982 and 0000 UTC 1, 2, 3 January 1987 were used to initialize the model runs. The choice of slightly different initial dates was arbitrary based on the availability of the data.

The observed SST anomaly for January 1983 (Fig. 1a) contains a very large warm anomaly across the central and eastern Pacific, with a maximum anomaly of over 4°C. The January 1987 SST anomaly (Fig. 1b) also contains a large region of warm water in the central and eastern Pacific, although the maximum magnitude is much less, about 1.5°C. The 1982/83 Pacific SST anomaly was of record magnitude, while that in 1986/87 was more typical, resembling in magnitude the composite El Niño anomaly of Rasmusson and Carpenter (1982). There were also appreciable and different extratropical Pacific SST anomalies in these two years as well (Fig. 1a,b). Although they were included in the experiments, no attempt has been made to account for their impact on prediction separately.

Of course the atmosphere and the GCM respond to the total SST rather than to the anomaly alone, and the area of intense convection in the tropical Pacific is strongly related to the area of very warm (28°–29°C) SST. In the January climatology used in the control experiments (Fig. 2a), this very warm water is confined to the west of 170°W along the equator. In January 1983, the 28°–29°C water extended across the entire Pacific basin due to the record magnitude of the anomalies (Fig. 2b). In January 1987, this very warm water is extended eastward relative to the climatology by about 30° longitude (Fig. 2c). Thus, one would expect the SST impact on prediction to be quite different between these two cases.

3. Results

In section 3a time mean observed and simulated anomalies are discussed for 1982/83 versus 1987. Root-mean-square (rms) errors and anomaly correlation coefficients (ACC) for the two years are presented in section 3b. To address questions raised concerning the SST impact on the extratropical circulation in these two years, the divergence and effective Rossby wave source fields are discussed in section 3c.

a. Time mean anomalies

Analysis of a large number of observed and simulated atmospheric fields for a wide range of time averages reveals that the impact on prediction due to the Pacific SST anomalies can best be seen on longer time averages on the order of 60 days. Thus, the anomaly maps presented in this section will all be time means for the first 60 days of the simulations. For the sake of brevity, SF will be referred to for 1982/83 figures when comparing with similar 1987 figures here.

Figure 3 depicts the observed and simulated precipitation anomalies for 1987 as does SF Fig. 7 for 1982/83. The observed precipitation anomalies (millimeters per day) are obtained by dividing the observed OLR anomalies (watts per square meter) by −5.7, an approximate empirical relation obtained by P. Arkin (1985, personal communication). All simulated anomalies depicted here are simply the average of the three boundary integrations minus the average of the three control integrations for the given year. The model climate drift is automatically removed from this type of anomaly, assuming the drift is the same in control and boundary integrations. Thus, this approach isolates the effect of the SST anomaly. In 1982/83 a large positive anomaly (4 mm day^{-1}) is observed across the

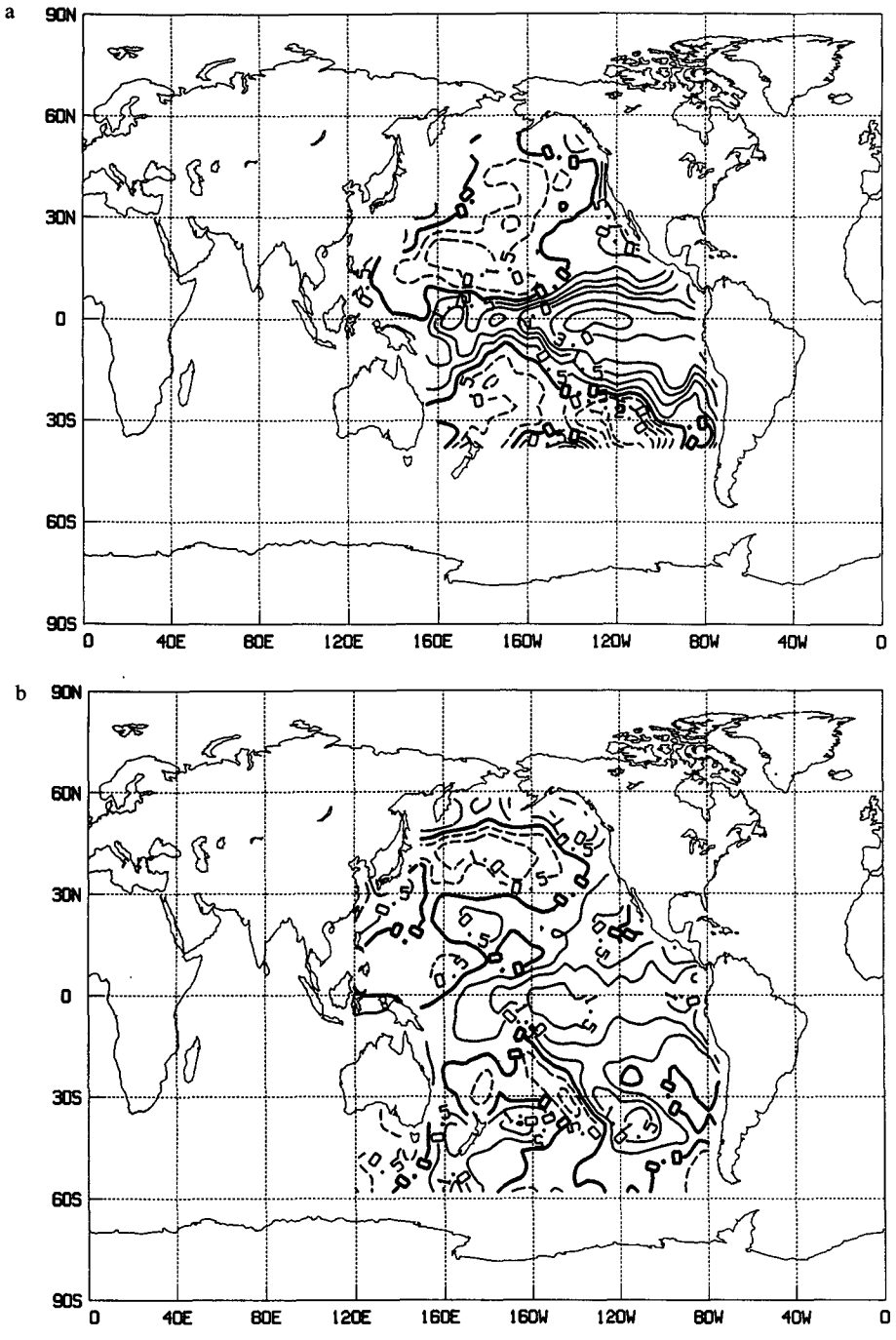

FIG. 1. Observed January sea surface temperature anomaly used for (a) 1983 and (b) 1987. Contours are ±1°, 1.5°, 2°, 3°, and 4°C. Dashed contours are negative.

entire central and eastern Pacific, with a maximum anomaly of over 12 mm day^{-1} in the vicinity of 150°W (SF, Fig. 7a). The positive anomaly in the simulated field greatly resembles that observed in both magnitude and position (SF, Fig. 7b), and it develops rapidly, even during the first five days of the integration. The model also simulates the large negative anomaly observed over Indonesia and Australia and the negative–positive anomaly dipole over Brazil. Overall, the simulation of the tropical precipitation anomalies in 1982/83 is very good. A large (4 mm day^{-1}) positive precipitation anomaly was also observed in 1987, although it is limited to the central Pacific and does not reach the magnitude of that observed in 1982/83 (Fig. 3a).

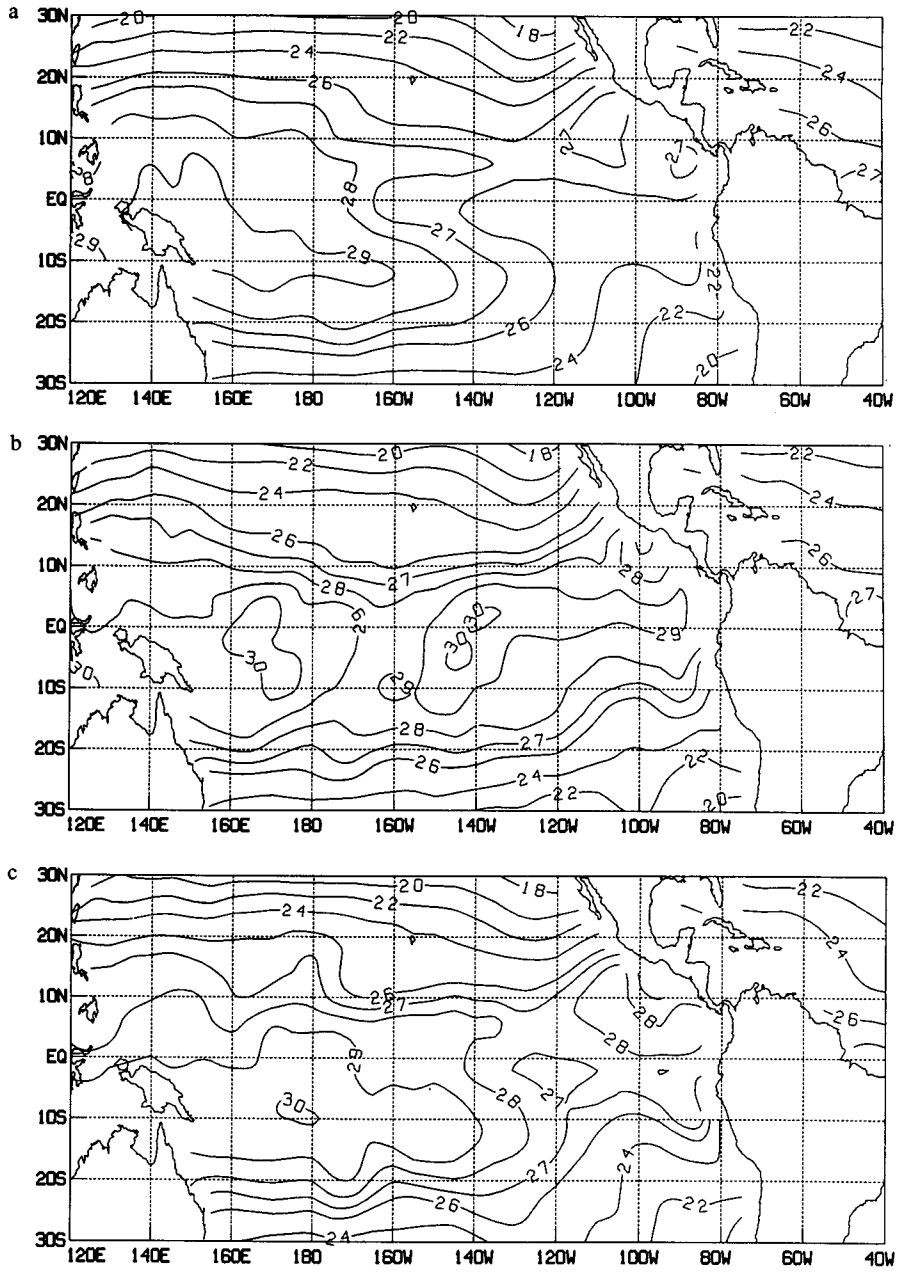

FIG. 2. January sea surface temperature for (a) climatology used in control integrations; (b) 1983 used in boundary integrations and (c) 1987 used in boundary integrations. Contours are 18°, 20°, 22°, 24°, 26°, 27°, 28°, 29°, and 30°C.

The model does a fair job of simulating this anomaly, although it positions it somewhat south of that observed. The model also simulates the negative–positive dipole observed over Brazil and the unusual positive anomaly over northern Australia. However, there is a very poor simulation of the main negative anomaly regions, with the model locating the main negative anomaly to the west of the large positive anomaly, while those observed are located north and south of the positive anomaly. Thus, the 1987 simulated precipitation anomalies bear some resemblance to those observed, but not to the extent that the 1982/83 simulated anomalies do. The simulated precipitation anomalies also took longer to develop in 1987, not completely organizing until roughly day 20 of the simulations (not shown).

The remainder of the observed anomalies discussed are formed by subtracting the mean of the NMC anal-

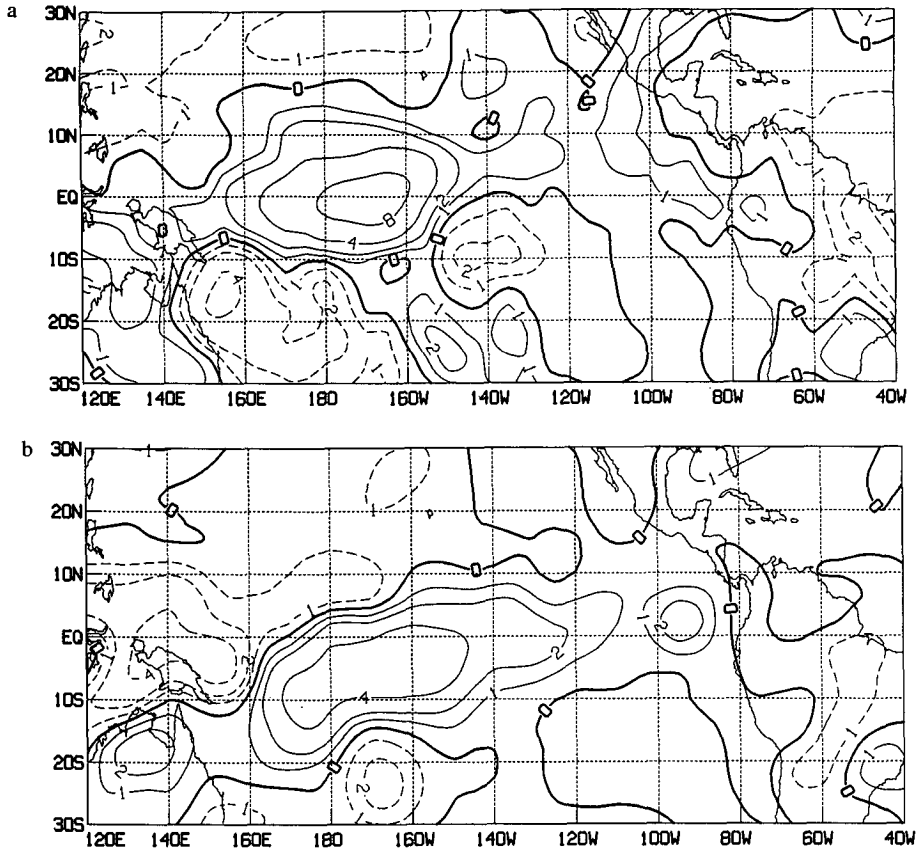

FIG. 3. Average precipitation for day 1–60 for 1987 for (a) observed anomaly calculated from observed OLR anomaly and (b) simulated anomaly. Contours are ±1, 2, 4, and 8 mm day^{-1}. Dashed contours are negative.

yses for January and February (JF) of 1979, 1980, 1981, 1982, and 1984 from the mean of the NMC analyses corresponding to the first 60 days of the model simulations.

The simulated 850-mb wind anomalies in the tropics (Fig. 4b) are consistent with the simulated anomalous moisture convergence (not shown), which greatly resembles the simulated anomalous precipitation (Fig. 3b). The observed 850-mb wind anomalies for JF 1987 contain a small region of modest (5 m s^{-1}) westerlies near the dateline just south of the equator (Fig. 4a). Anomalous winds converge in this region from the north and the south, consistent with the moisture supply regions seen in the observed precipitation anomaly (Fig. 3a). The simulated 850-mb wind anomaly field lacks both this north–south convergence and the associated anticyclonic anomalies on either side of the equator (Fig. 4b). The simulations also contain equatorial westerly anomalies that are both stronger and more widespread than those observed. In 1982/83 both the observed and simulated 850-mb wind fields contained a wide region of strong (10 m s^{-1}) westerly anomalies in the central Pacific (SF, Fig. 8a,b). Thus the regions of low-level wind and moisture divergence simulated in 1987 bear more resemblance to those observed in 1982/83 than those observed in 1987, even though the 1987 positive precipitation and moisture convergence anomalies are relatively well simulated. The models preference for moisture divergence from the western Pacific may be related to problems with its climatology, which contains overly intense precipitation in this region (SF, Fig. 4b). An analysis of the 30-day mean 850-mb wind anomalies for 1987 reveals that the model maintained westerly anomalies throughout the entire period, while westerly anomalies were observed only during the second 30 days (not shown). In 1982/83 strong westerly anomalies are both observed and simulated throughout the 60-day period.

In 1982/83 the GCM correctly simulates a strong negative phase of the Southern Oscillation (SO) in the 60-day mean tropical sea-level pressure (SLP) field, with the eastern Pacific being roughly 2 mb below normal and the western Pacific 2 mb above normal (SF, Fig. 9a,b). The model also correctly simulates the observed SO signal in 1987, which was half the magnitude of that in 1982/83 (not shown). As with the precipi-

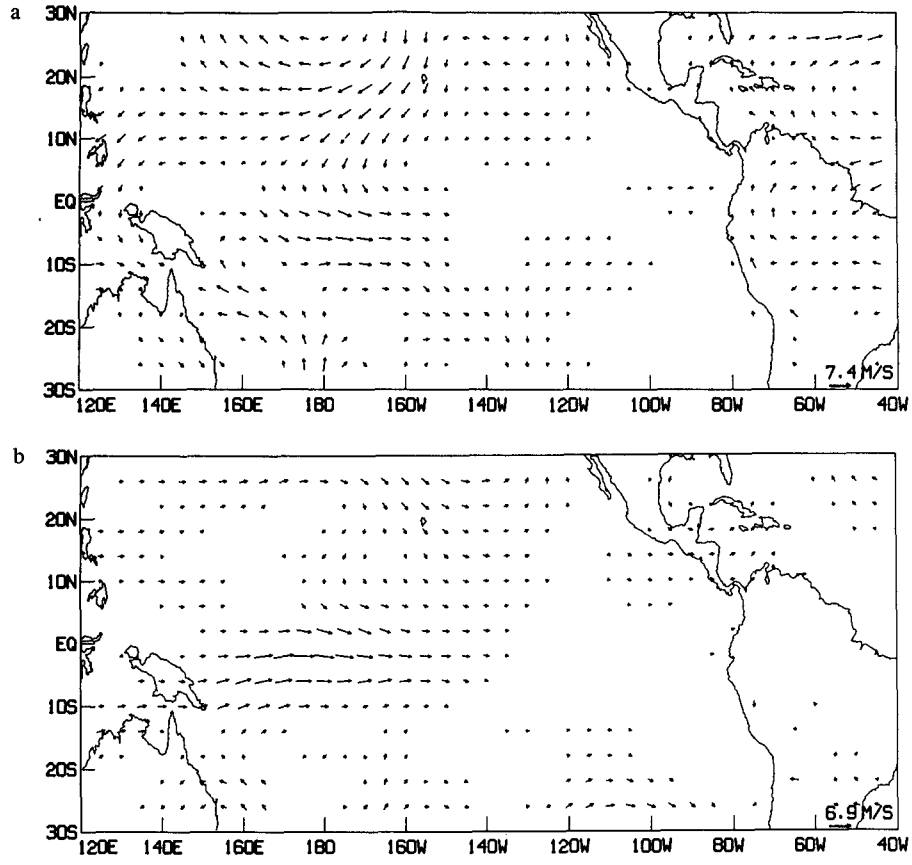

FIG. 4. Average 850-mb wind vectors for day 1–60 for 1987 for (a) observed anomaly and (b) simulated anomaly. Arrow at bottom gives scale in meters per second.

tation anomalies, this signal took two to three weeks to develop in the 1987 simulations as opposed to its almost immediate development in 1982/83.

Well-simulated easterly anomalies in the 60-day mean 300-mb wind over the central equatorial Pacific are much weaker in 1987 (5 m s^{-1}) than in 1982/83 (15 m s^{-1}, not shown). Straddling westerly anomalies at 30°N and 30°S are also well simulated in 1982/83 (10 m s^{-1}) and 1987 (5 m s^{-1}).

The observed and simulated anomalies in the zonal departure of 200-mb streamfunction for 1982/83 and 1987 are shown in Figs. 5 and 6, respectively. The observed anomaly for 1982/83 contains a strong anticyclonic couplet straddling the equator in the central and eastern Pacific and a weaker cyclonic couplet downstream in the tropics (Fig. 5a). These features are well simulated by the model, although their magnitude is a little weak (Fig. 5b). Over the Pacific and North America an eastward shifted PNA-like pattern (Wallace and Gutzler 1981) is present in both the observed and simulated anomaly fields. In 1987, an anticyclonic couplet is also observed straddling the equator in the central Pacific, but it is smaller, weaker, and westward of that observed in 1982/83 (Fig. 6a). The model correctly simulates this feature, although the center of the northern anticyclonic cell is somewhat northwest of that observed (Fig. 6b). The model also simulates the downstream cyclonic couplet observed in the tropics, which was also weaker than that in 1982/83. In 1987, a PNA-like pattern somewhat similar to that in 1982/83 is observed, although the 1987 pattern is not shifted as far eastward and the low over the Gulf of Mexico and Florida has been replaced by two lows to the east and west. In addition, a positive anomaly is present in the vicinity of Greenland and Iceland instead of the negative anomaly observed in 1982/83. The model correctly simulates much of this 1987 pattern, but it forecasts a single low over the Gulf of Mexico and Florida instead of the split low observed. Overall, the simulated 1987 extratropical features show some correspondence to those observed, although perhaps not as well as do the 1982/83 simulations. It is interesting that the observed and simulated extratropical features have the same magnitude and contain similar patterns in these two years. However, differences between the two years can easily be seen in the difference of the observed 60-day mean 300-mb geopotential for 1987 minus 1982/83 (Fig. 7a). The corresponding difference

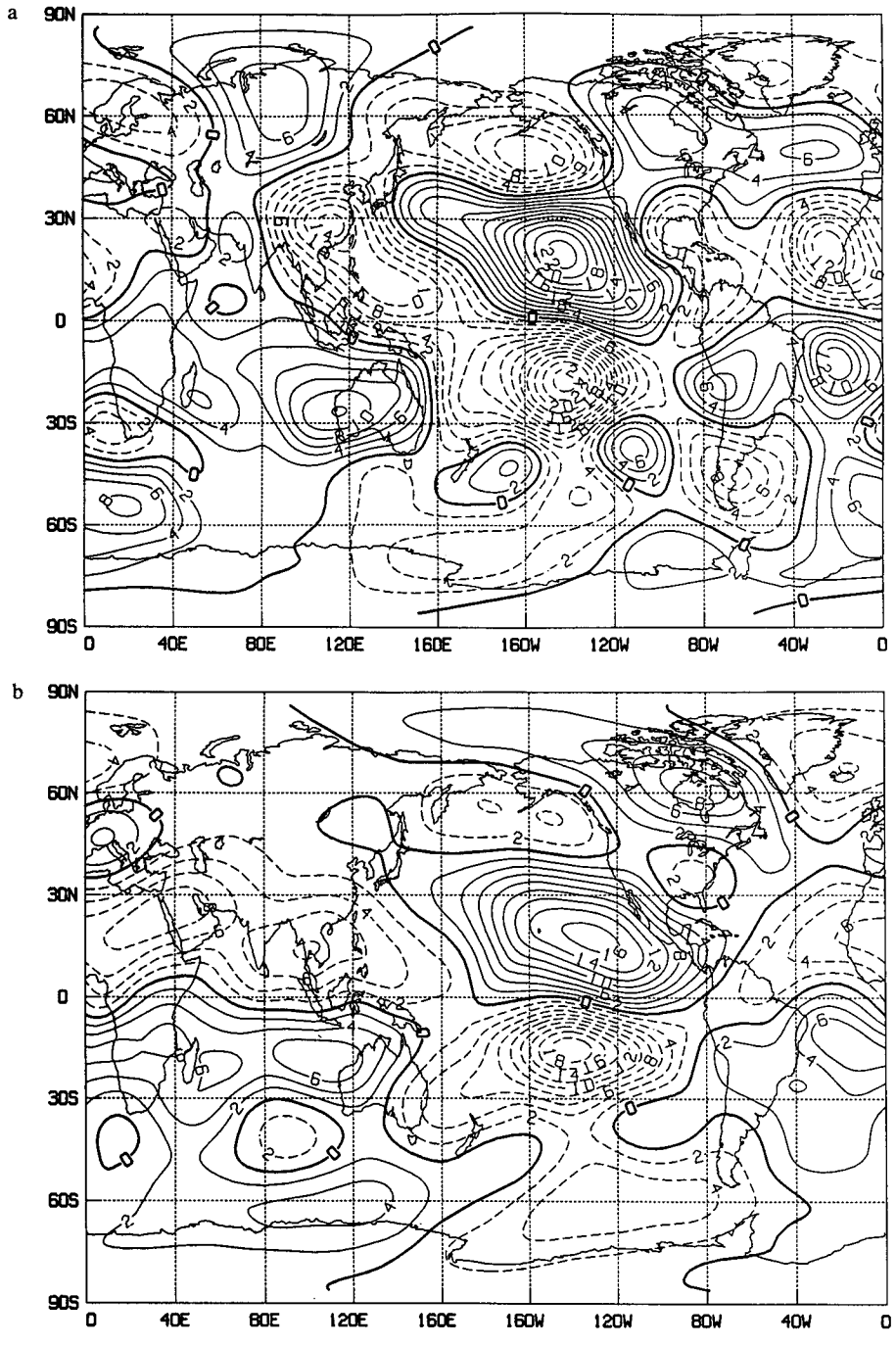

FIG. 5. Average zonal departure of 200-mb stream function for day 1–60 for 1982/83 for (a) observed anomaly and (b) simulated anomaly. Contour interval is 2×10^6 m^2 s^{-1}. Dashed contours are negative.

between the boundary simulations contains many of the major observed differences, including the positive–negative dipole over Greenland and the North Atlantic, the negative difference over northwestern Eurasia, the band of positive differences in the Southern Hemisphere midlatitudes, and the widespread negative difference throughout the tropics (Fig. 7b). It is important to note that this difference between the boundary simulations may include features that are dynamically related to the observed initial atmospheric state in each year, in addition to features related to the SST. The dynamical memory of planetary waves contained in

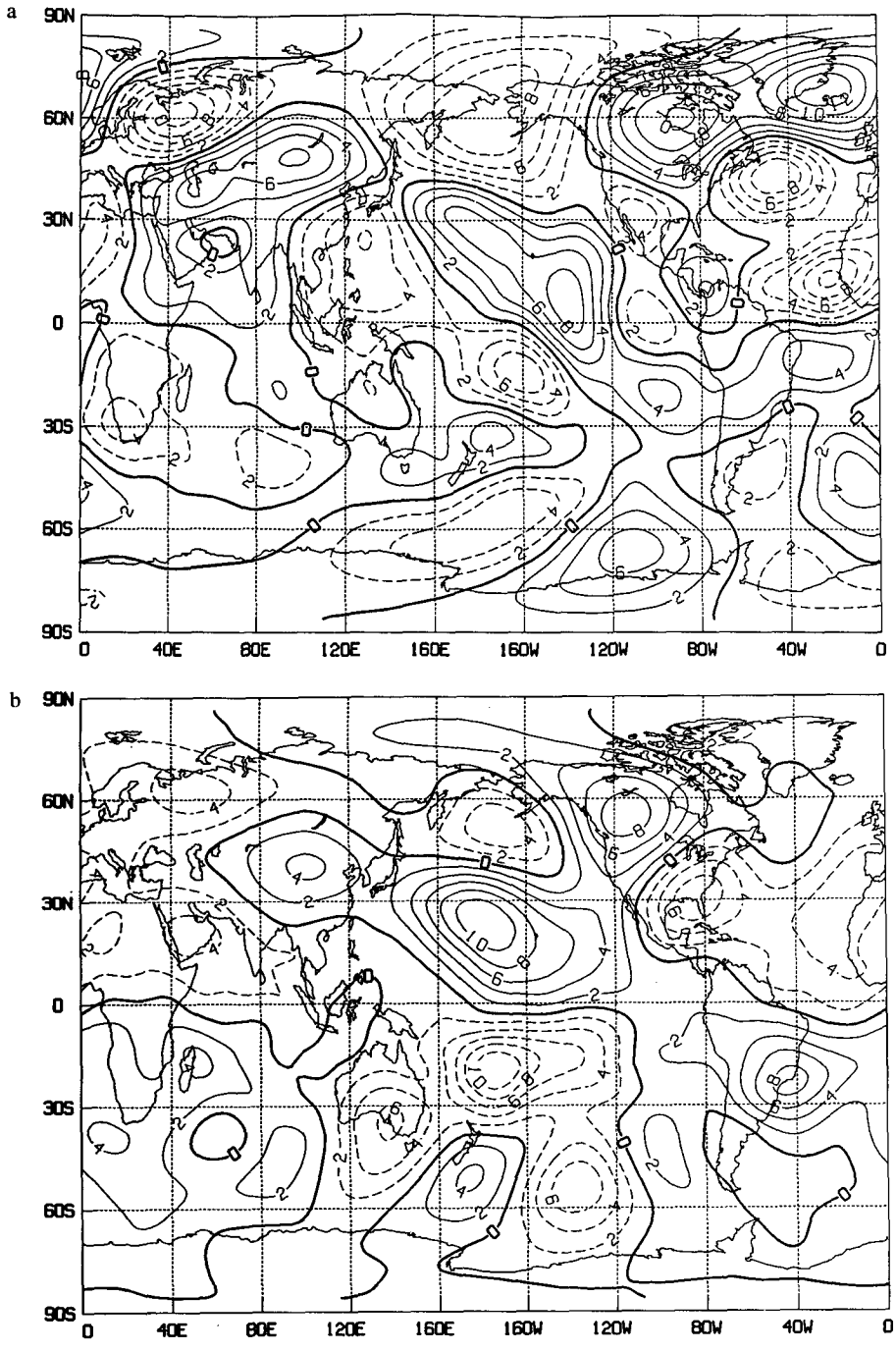

FIG. 6. Average zonal departure of 200-mb streamfunction for day 1–60 for 1987 for (a) observed anomaly and (b) simulated anomaly. Contour interval is 2×10^6 m^2 s^{-1}. Dashed contours are negative.

the initial state can contribute to longer-term predictability due to the extended predictability of planetary waves and the fact that planetary waves contribute most to monthly means (Shukla 1981). Thus, it is not surprising that the GCM appears to do a better job at simulating the differences between these two years than it does at simulating all the observed anomalies in a given year via the inclusion of the observed SST anomalies alone. The ability of the GCM to simulate these differences is encouraging.

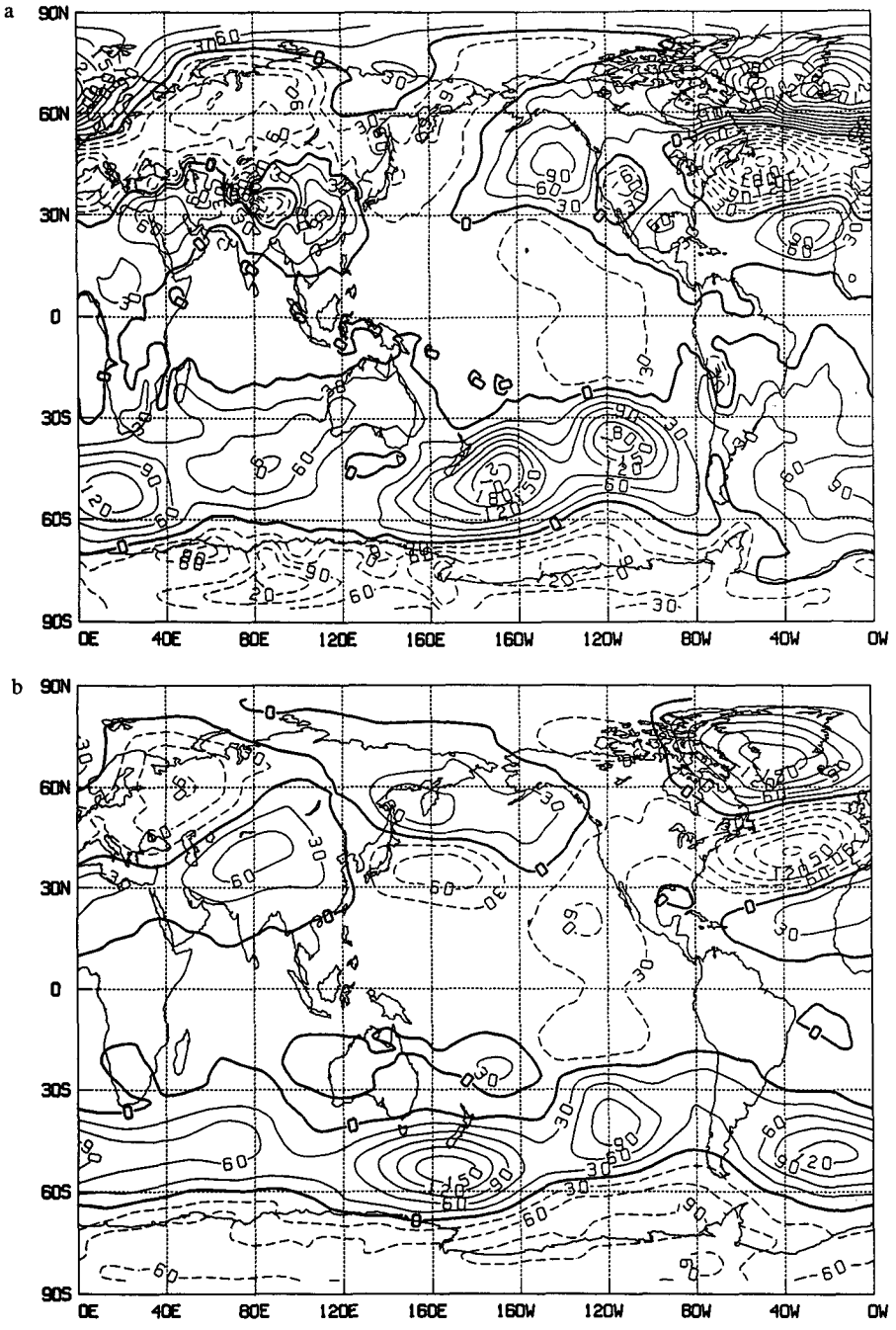

FIG. 7. Average 300-mb geopotential height difference for day 1–60: 1987 minus 1982/83, for (a) observations and (b) boundary integration ensemble. Contour interval is 30 m. Dashed contours are negative.

b. Skill scores

An overall picture of how the observed SST anomalies impacted the time mean forecasts for different areas can be seen in the 10-day mean rms error of 300-mb geopotential (Fig. 8). The ensemble mean of the three control forecasts is shown as a dashed curve, while that for the three boundary forecasts is shown as a solid curve. It should be noted that a given geopotential height difference is more significant in low latitudes than in high latitudes. The following discussion will focus on the change in rms error due to the influence

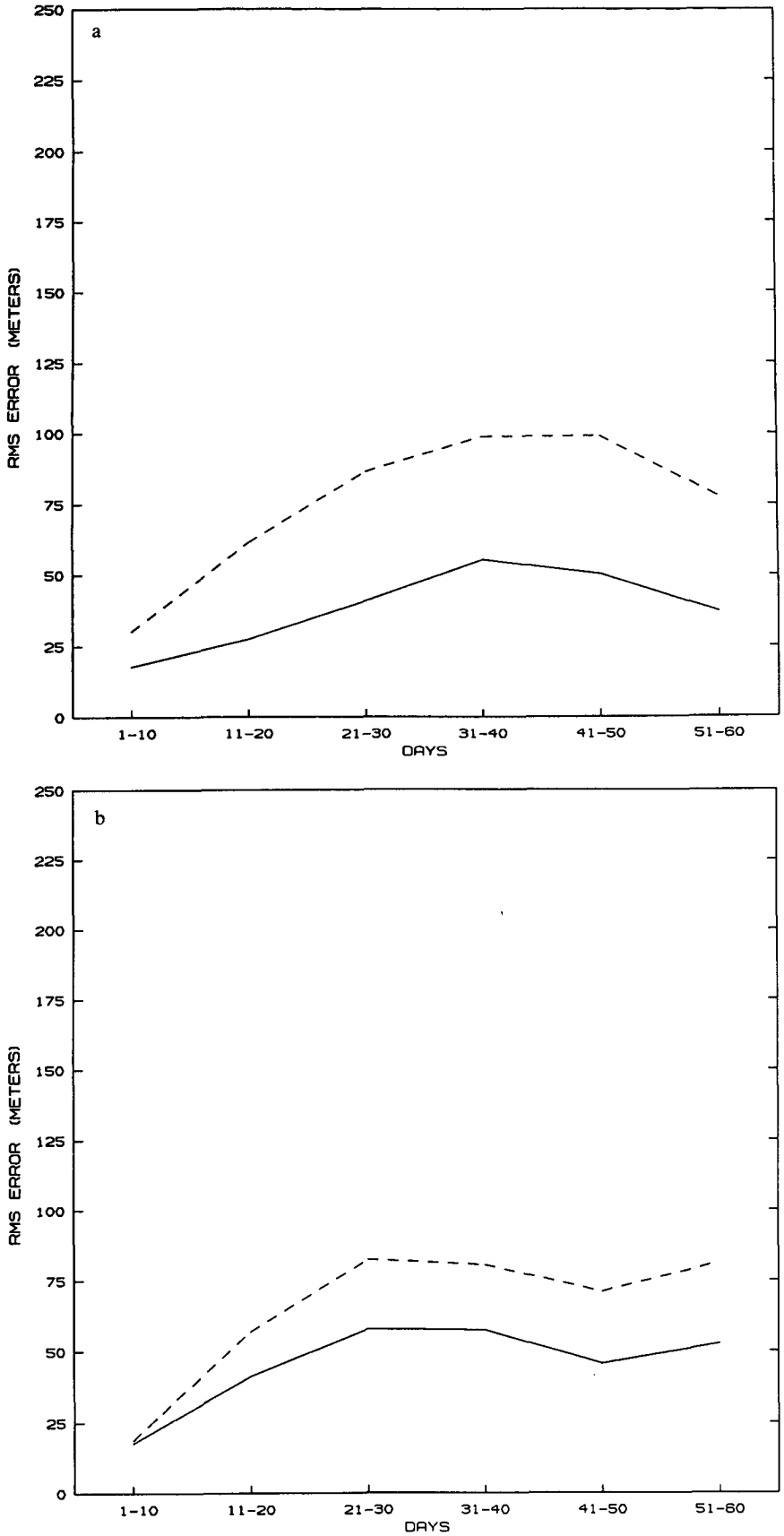

FIG. 8. Ten-day mean error (meters) for (a) 1982/83 tropics (20°S–20°N); (b) 1987 tropics; (c) 1982/83 Northern Hemisphere (20°–76°N); and (d) 1987 Northern Hemisphere. Control ensemble is dashed; boundary ensemble is solid.

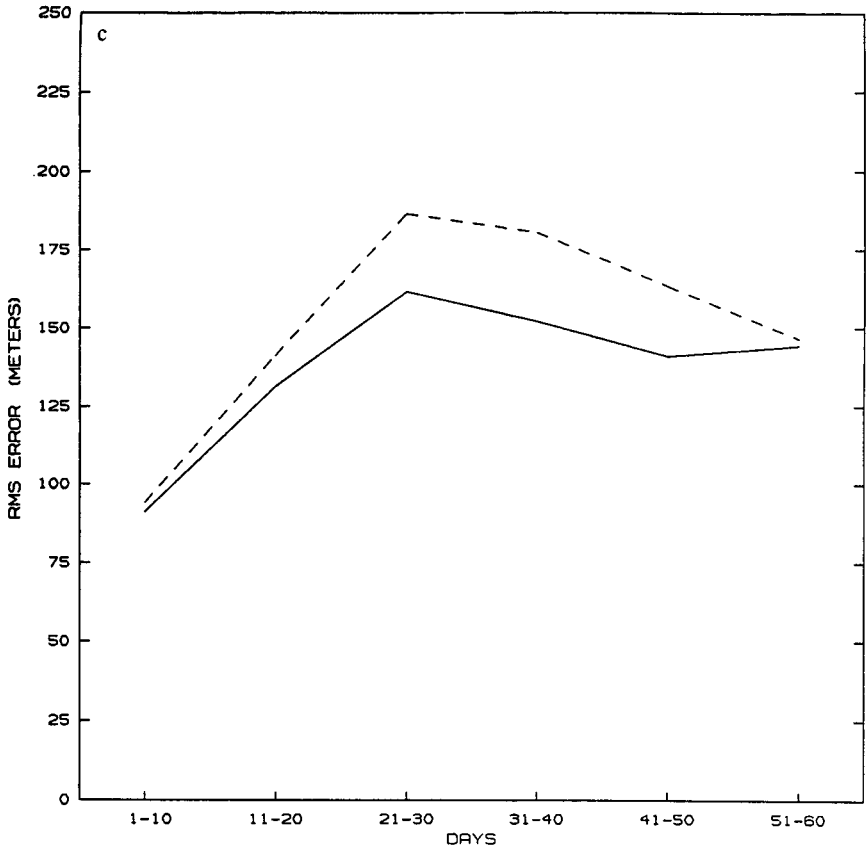

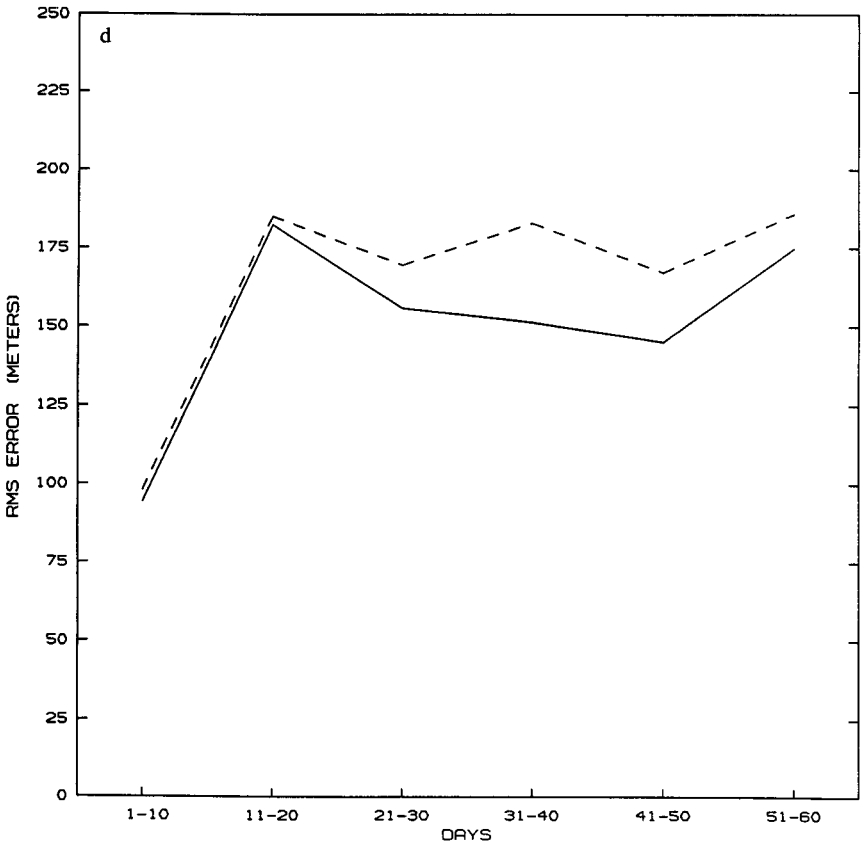

FIG. 8. (*Continued*)

of SST relative to the magnitude of the rms error in the same region of the control simulation. In the tropics (20°S–20°N) a large increase in skill develops almost immediately for 1982/83, roughly halving the rms error (Fig. 8a). In 1987, the tropical rms error is also largely improved in the boundary simulations, although this improvement did not develop so quickly and is only half the magnitude of that in 1982/83 (Fig. 8b). The 1982/83 rms error in the Northern Hemisphere (NH, 20°–76°N) shows a modest forecast improvement upon including the observed SST (Fig. 8c); however, this improvement is realized in each of the component members of the ensemble (not shown). In 1987, there is no forecast improvement in the first 20 days in the NH, followed by a modest improvement for the remainder of the experiment (Fig. 8d). This improvement in 1987 is not so reproducible as that in 1982/83 having occurred in only two of the three members of the ensemble. The 10-day mean time series of 300-mb geopotential anomaly correlation coefficients (ACC, not shown) reflects these same tropical and NH features, as does the 30-day mean rms error and ACC for 1982/83 (Table 1a,b) and 1987 (Table 1c,d). In Table 1, the 30-day mean tropical and NH scores are given for each initial condition as well as for the ensemble average for both the control (CON) and boundary (BOU) simulations. In 1982/83 (Table 1a,b) there is a large SST impact on the tropical scores and a modest impact on the NH scores. This positive impact in 1982/83 occurred in the 1–30 day mean as well as in the 31–60 day mean. In 1987 (Table 1c,d) the SST impact took longer to develop. The 1–30 day mean scores for 1987 show a modest SST impact on the tropical scores but little or no impact on the NH scores. However, the 30–60 day mean scores for 1987 display an impact similar to that seen in 1982/83. In both years the tropical ACC scores for the control simulations are negative, due to the combined effects of an incorrect simulation of the large-scale circulation and a strong negative model bias. In fact, the model bias is so strong that for the 1987 case even the moderate SST anomalies could not produce a positive tropical ACC for the boundary simulations.

Although the positive forecast impact of the SST is present in relatively short time means (i.e., 10 days, Fig. 8), we were interested to find out if this impact simply persists for the whole 60 days or if there is also improvement in the prediction of individual 10-day means beyond that of the 60-day mean impact. For this purpose, we first removed the 60-day means and

TABLE 1. The 300-mb geopotential root-mean-square (rms) error (meters) and anomaly correlation coefficient (ACC) for control integrations (CON) and boundary integrations (BOU) for days 1–30 and 31–60.

Initial condition	Tropics (20°S–20°N)				Northern Hemisphere (20°N–76°N)			
	1–30		31–60		1–30		31–60	
	CON	BOU	CON	BOU	CON	BOU	CON	BOU
				A. 1982/83 rms				
15 December 1982	54	25	93	40	121	114	155	137
16 December 1982	55	24	89	50	125	110	149	130
17 December 1982	58	30	93	50	118	115	149	131
Ensemble	58	27	91	46	122	112	138	120
				B. 1982/83 ACC				
15 December 1982	−0.53	0.75	−0.75	0.56	0.15	0.19	0.18	0.42
16 December 1982	−0.53	0.76	−0.69	0.21	−0.05	0.24	0.37	0.43
17 December 1982	−0.53	0.61	−0.76	0.23	0.06	0.24	0.41	0.48
Ensemble	−0.60	0.71	−0.75	0.35	0.00	0.18	0.36	0.49
				C. 1987 rms				
1 January 1987	44	29	78	46	124	117	155	122
2 January 1987	43	31	71	53	124	126	154	144
3 January 1987	49	34	80	52	126	131	142	135
Ensemble	49	33	76	50	124	122	144	125
				D. 1987 ACC				
1 January 1987	−0.47	0.29	−0.74	−0.28	0.24	0.32	0.16	0.45
2 January 1987	−0.43	0.20	−0.73	−0.48	0.25	0.26	0.23	0.39
3 January 1987	−0.57	0.07	−0.75	−0.35	0.18	0.21	0.37	0.26
Ensemble	−0.58	0.04	−0.75	−0.38	0.21	0.26	0.24	0.36

then examined the skill scores for individual 10-day averages. We found that most of the forecast improvement is indeed present in the longer time scale average of 60 days. This result is evident in a large variety of fields and time means and is quantified by the skill scores in Table 2, discussed in the following text.

Table 2 summarizes the SST impact on the forecast ensembles for 1982/83 and 1987 for different time means. The 300-mb geopotential rms error for the control ensemble is given in lightface (CON), with the corresponding mean percentage improvement over this score obtained in the SST boundary ensemble in boldface (%). These 2 numbers are given for the mean of the 6 10-day scores (1–10, 11–20, . . .), the mean of the 4 30-day scores (1–30, 11–40, . . .), and the 60-day mean. Note that the rms erros and percentage improvements are calculated for each 10 (30)-day time period first and then averaged to obtain the mean rms error and mean percentage improvement for all 10 (30)-day time means. Values are given for 1) the total time mean field (TOTAL) and 2) the deviation of the 10- or 30-day mean total field from the 60-day mean total field (DEV60). In each case the scores are calculated by verifying the forecast ensembles against the equivalent observed component of the geopotential. The results discussed here are also reflected in the anomaly correlation coefficients (not shown).

In the tropics (20°S–20°N, Table 2a) there is a slight trend for better control rms scores and larger SST impact for longer time means in both years. There is a roughly 50% improvement in the total scores in 1982/83 versus a 30% improvement in 1987 due to the SST. The relative improvements in the DEV60 components are smaller, roughly 20% in each year. Comparing the improvement in the 60-day TOTAL rms to the improvement in the 10- and 30-day DEV60 rms reveals that the major SST impact in the tropics occurs for longer time scales.

In the Northern Hemisphere (NH, 20°–76°N, Table 2b) there is a trend for better rms scores and larger SST impact for longer time means in both years; however, the actual impact is quite small. The total scores improved by just over 10% in 1982/83 and by just under 10% in 1987 due to the SST impact. The percentage improvement in the DEV60 scores is somewhat smaller, once again reflecting the relatively larger SST impact on longer time scales. The scores for the Southern Hemisphere (SH, 20°–76°S, Table 2c) are similar to those in NH, although the SST impact is somewhat smaller in both years.

The overall similarity of the SST impact in the extratropics in 1982/83 versus 1987 is striking considering the different SST impacts in the tropics in these two years. To investigate this apparently nonlinear relation between the tropical and extratropical circulation anomalies, we analyze the observed and simulated divergence and effective Rossby wave source fields in these two years in section 3c.

TABLE 2. The control integration ensemble 300-mb geopotential root-mean-square error (CON, meters) and the percentage improvement in the boundary integration ensemble (%) for the total field (TOTAL) and the deviation from the 60-day mean (DEV60).

		1982/83			1987		
	Run	10 day	30 day	60 day	10 day	30 day	60 day
		A. Tropics (20°S–20°N)					
TOTAL	CON	76	81	75	65	68	62
	(%)	*49*	*51*	*53*	*27*	*32*	*34*
DEV60	CON	25	16		28	15	
	(%)	*16*	*27*		*17*	*21*	
		B. Northern Hemisphere (20°N–76°N)					
TOTAL	CON	152	142	121	165	142	126
	(%)	*9*	*12*	*12*	*8*	*9*	*10*
DEV60	CON	96	49		108	47	
	(%)	*8*	*5*		*7*	*1*	
		C. Southern Hemisphere (20°S–76°S)					
TOTAL	CON	133	125	119	149	144	131
	(%)	*7*	*7*	*8*	*4*	*8*	*8*
DEV60	CON	69	38		80	46	
	(%)	*5*	*6*		*−6*	*−7*	

c. *Divergence and Rossby wave source*

Held and Kang (1987) have shown that convergence in the northern subtropical central Pacific is more important than direct tropical divergence forcing in obtaining the wavetrainlike response of a GFDL GCM to El Niño SST anomalies. In light of the very different tropical forcing and yet somewhat similar extratropical responses obtained in the two cases discussed here, it seems appropriate to examine both the tropical and subtropical forcings by examining the anomalous divergence as did Held and Kang (1987). As a note of caution we point out that the observed anomalous divergence fields shown here are calculated from NMC analyses for the years previously described. These analyses may have underestimated the magnitude of the divergence field, particularly in the earlier years (Trenberth and Olson 1988).

The observed 60-day mean anomalous 200-mb divergence field for 1982/83 contains a region of divergence over the central and eastern tropical Pacific from roughly 20°S to 20°N (Fig. 9a). A large region of anomalous convergence is observed to the west from the dateline to 120°E and from 20°N to 20°S over the region of reduced precipitation. A large region of strong anomalous convergence is observed to the north in the central Pacific centered on 30°N. The corresponding simulated anomaly (Fig. 9b) also contains a region of divergence over the central and eastern tropical Pacific, although it is much more intense and is constrained

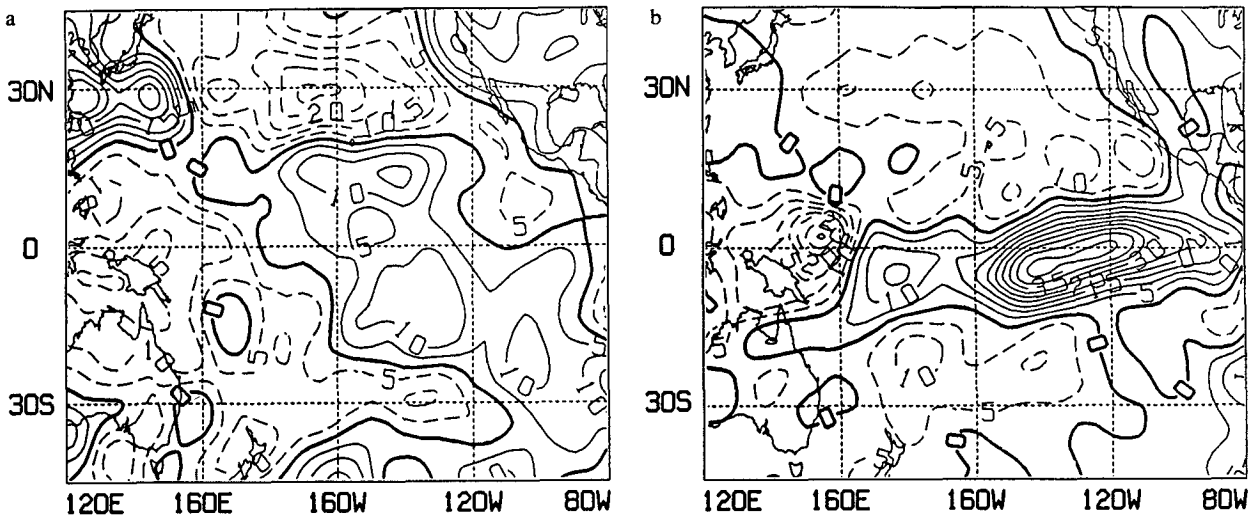

FIG. 9. Average 200-mb divergence for day 1–60 for 1982/83 for (a) observed anomaly and (b) simulated anomaly. Contour interval is 5×10^{-7} s^{-1}. Dashed contours are negative.

more latitudinally than that observed. The simulated region of intense convergence to the west along the equator is also limited in its latitudinal extent compared to that observed. A region of relative convergence is simulated in the vicinity of 30°N in the central Pacific; however, it is weaker and extends southward compared to that observed.

The observed anomalous 200-mb divergence field for 1987 contains a region of intense divergence in the central tropical Pacific which extends to the west-southwest over Indonesia and northern Australia (Fig. 10a). We believe that the larger magnitude of the 1987 observed tropical divergence anomaly compared to that in 1982/83 could be due to an improved NMC analysis of tropical divergence in 1987. A strong region of convergence in the central Pacific centered on 30°N resembles that observed in 1982/83, although it does not extend as far to the east as that in 1982/83. The 1987 simulated anomalous divergence field contains a region of strong divergence along the equator which resembles that observed, although its westward extension is farther south and too weak compared to that observed (Fig. 10b). The incorrect simulation of a region of convergence in the vicinity of Indonesia reflects deficiencies in the anomalous precipitation simulation noted previously. An area of convergence in the vicinity of 30°N in the central Pacific is well situated albeit weak compared to that observed.

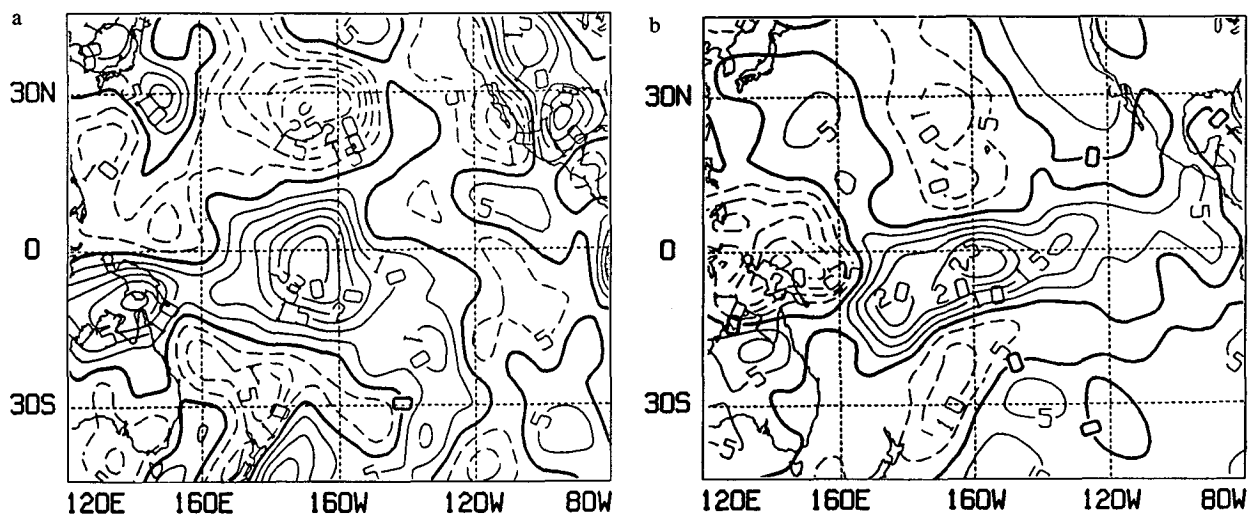

FIG. 10. Average 200-mb divergence for day 1–60 for 1987 for (a) observed anomaly and (b) simulated anomaly. Contour interval is 5×10^{-7} s^{-1}. Dashed contours are negative.

Given the similar magnitude and somewhat similar character of the observed and simulated extratropical anomalies in these two years (Figs. 5 and 6), one might expect the dominant forcing of these anomalies to be somewhat similar. The feature most similar between the two years in the observations is the area of subtropical convergence in the vicinity of 30°N in the central Pacific (Figs. 9a and 10a). The observed convergence anomalies in this area are very similar, apart from an eastward extension in 1982/83 by 15 degrees relative to that in 1987. The simulated convergence anomalies also differ in this same way, although both are too weak compared to those observed. Given that the simulated extratropical response is also too weak in these two cases (Figs. 5b and 6b), the Held and Kang conclusion concerning the dominance of forcing from the subtropical central Pacific in forcing the GFDL GCM also appears to be a plausible explanation for the GLAS GCM responses in these two cases. However, as pointed out by Sardeshmukh and Hoskins (1988), when diagnosing the forcing of extratropical wave trains, it is not sufficient to examine the anomalous divergence alone, and the full effective Rossby wave source (S) should be considered. The term S is defined by Sardeshmukh and Hoskins (1988) as

$$S = -\mathbf{v}\cdot\nabla\zeta - \zeta D \qquad (1)$$

where $\mathbf{v}$ is the divergent component of the wind, ζ is the absolute vorticity, and D is the divergence. Examining only the divergence field as a forcing for the extratropics ignores both the vorticity factor in the second (stretching) term on the right-hand side of Eq. (1), as well as the entire first term on the right-hand side of Eq. (1), which represents the advection of absolute vorticity by the divergent wind.

The quantity S was calculated and examined for each of the control ensembles, boundary ensembles, observed climatology, and observations for each of the two years considered here. As with all the previously shown fields, these calculations were done on 60-day means. Rather than show twice as many maps and discuss the differences between control and boundary maps of S, the differences of boundary S minus control S are compared to observed S minus observed climatological S for each year. These differences will be referred to as the simulated and observed anomalous S. The 200-mb observed anomalous S for 1982/83 contains a relatively weak signal in the tropics and a strong positive signal in the vicinity of 30°–40°N in the central Pacific (Fig. 11a). The corresponding simulated field has somewhat different weak tropical signals, but as its strongest feature it has a positive signal in the subtropical central Pacific that is quite similar to that observed but of roughly half the magnitude (Fig. 11b).

In 1987 the strongest signal in the 200-mb observed anomalous S field is also in the subtropical central Pacific in the vicinity of 30°–40°N. This signal is of the same magnitude as that observed in 1982/83, although it is considerably more limited in its longitudinal extent and is flanked to the east by a negative signal (Fig. 12a). This feature is well simulated, although again the magnitude is half that observed (Fig. 12b). The well-situated but reduced magnitude anomalous S simulated in the central subtropical Pacific in these two cases is consistent with the weaker than observed simulated wavetrains.

We have also examined the contribution of each of the two terms in Eq. (1) to the anomalous S in these two years. In the region considered (Figs. 9–12), the stretching term dominates the signal in S in both the observations and the simulations (not shown).

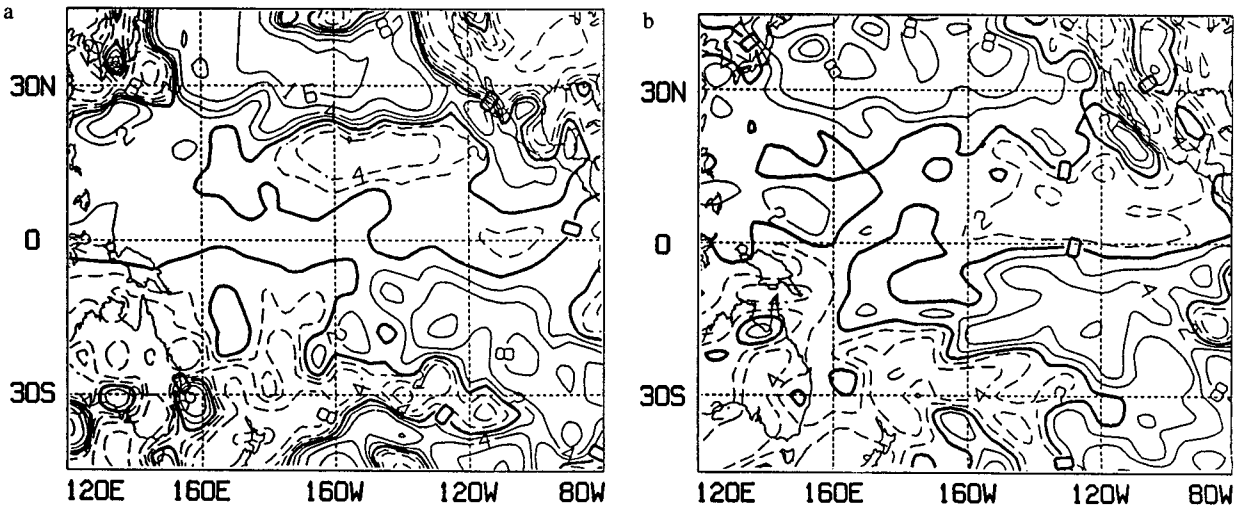

FIG. 11. Average 200-mb effective Rossby wave source for day 1–60 for 1982/83 for (a) observed anomaly and (b) simulated anomaly. Contour interval is 2×10^{-11} s^{-2}. Dashed contours are negative.

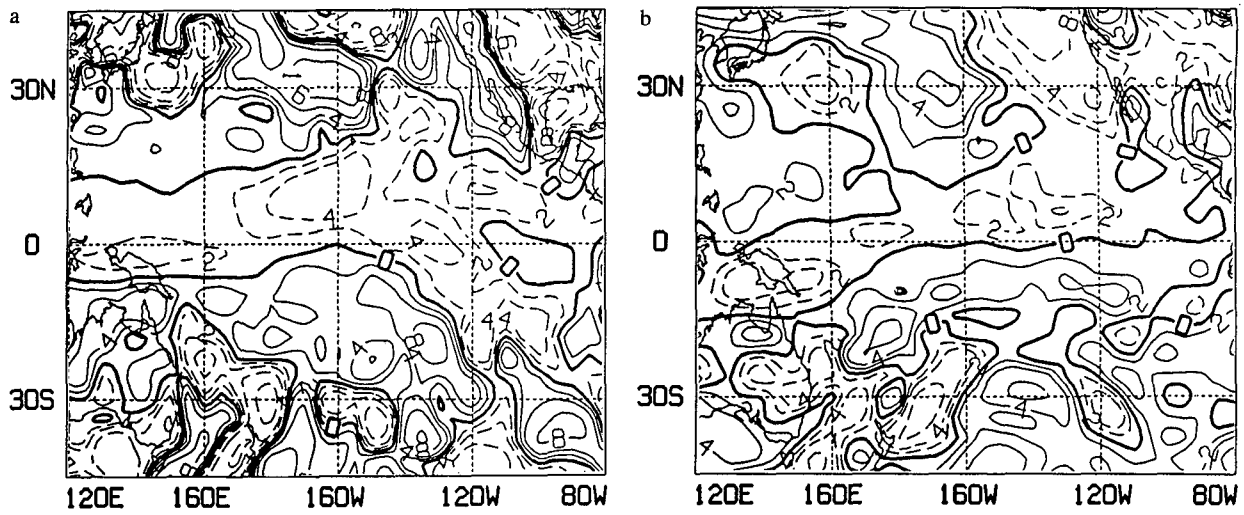

FIG. 12. Average 200-mb effective Rossby wave source for day 1–60 for 1987 for (a) observed anomaly and (b) simulated anomaly. Contour interval is 2×10^{-11} s^{-2}. Dashed contours are negative.

4. Discussion

Earlier studies have shown that the record 1982/83 El Niño Pacific SST anomalies are capable of producing a positive impact on predictions with a GCM in both the tropics and the extratropics. Results from simulations with the 1986/87 Pacific SST anomalies show that a positive impact on prediction can occur even when the SST anomalies are of more typical magnitude. This finding is encouraging due to the relatively frequent occurrence of moderate El Niño SST anomalies and the prospect of predicting them with a coupled atmosphere–ocean model.

Although a positive forecast impact is obtained by including the Pacific SST anomalies from both of these two years, important differences in this impact are seen. The observed and simulated time mean anomalies in the tropics are much larger in 1982/83 than in 1987. The impact of including the observed SST anomalies on the forecast skill scores in the tropics is also much larger in 1982/83. Thus, the impact of the observed SST anomalies on prediction in the tropics does seem related to the strength of the SST anomalies. In 1982/83 the SST anomalies were large enough to extend the region of very warm (29°C) water, normally confined to the western equatorial Pacific, across the entire equatorial Pacific basin. In 1987, as in the composite case of Rasmusson and Carpenter (1982), the SST anomalies merely extend this very warm water a little eastward into the central equatorial Pacific. This region where the very warm equatorial water has been extended is where the major anomalous convection and heating occur in both the observations and the GCM. Thus, the region of anomalous heating is much larger in 1982/83 than in 1987, and the tropical forecast impact is much larger. The strength of the SST anomalies also affects the response time of the GCM, with a positive forecast impact developing more rapidly in 1982/83 than in 1987 in both the tropics and the extratropics. The surface latent heat flux, moisture convergence, and precipitation anomalies in the immediate vicinity of the positive tropical SST anomalies developed much faster in 1982/83 than in 1987, thus, driving the rest of the model response. We believe this is because of the larger SST anomalies producing larger and faster positive feedbacks between anomalous moisture convergence and anomalous heating. Nevertheless, the SST impact on prediction occurred mainly on longer time scales (60 days) in both the tropics and the extratropics in both years.

The forecast impact in the extratropics does not seem to be well related to the strength of the SST anomalies or even the strength and expanse of the tropical heating and divergence anomalies. A modest forecast improvement occurred in the extratropics in both 1982/83 and 1987, slightly more in 1982/83. The time mean simulated anomalies also resemble their observed counterparts somewhat better in 1982/83 than in 1987. We examined the anomalous divergence and anomalous effective Rossby wave source (S) in the tropics and subtropics for these two years. In both the observations and the simulations, the largest signals in S are in the northern subtropical Pacific, not the tropics. This region of anomalous S is of similar magnitude for the two years, although the pattern, which is fairly well simulated in each year, is somewhat different between the two. In each year, the simulated anomalous S in this region is somewhat weaker than that observed, consistent with the weaker than observed GCM extratropical wave train over the Pacific and North America. Thus although we cannot determine cause and effect by examining S diagnostically, we speculate that this wavetrain response could be forced from the subtropical Pacific, in agreement with the results of Held and

Kang (1987) for a GFDL GCM. Of course, this subtropical anomaly itself could have been forced either directly or indirectly by the SST anomalies. Held et al. (1989) have shown that such subtropical anomalies may be forced by transients, which, in turn, are subject to alteration by the anomalous SST. Due to the small magnitude of the SST anomalies in the central subtropical Pacific, we further speculate that the simulated anomalies in this region were forced from the tropics.

Acknowledgments. The authors would like to thank Ms. Diane Marciso of CAC for providing the SST anomalies used in this study. We are grateful to Ms. Marlene Schlichtig for her careful preparation of the manuscript. This research was supported by the NASA climate program (NAGW-557) and NSF Grant ATM-8414660.

REFERENCES

Arakawa, A., 1969: Parameterization of cumulus convection. *Proc. of the WMO/IUGG Symp. on Numerical Prediction.* Tokyo, WMO, 1–6.

Deardorff, J. W., 1972: Parameterization of the planetary boundary layer for use in general circulation models. *Mon. Wea. Rev.*, **100,** 93–106.

Fennessy, M. J., and J. Shukla, 1988: Numerical simulation of the atmospheric response to the time-varying El Niño SST anomalies during May 1982 through October 1983. *J. Climate,* **1,** 195–211.

——, L. Marx and J. Shukla, 1985: General circulation model sensitivity to 1982/83 equatorial Pacific sea surface temperature anomalies. *Mon. Wea. Rev.*, **113,** 858–864.

Geisler, J. E., M. L. Blackmon, G. T. Bates and S. Munoz, 1985: Sensitivity of January climate response to the magnitude and position of equatorial Pacific sea surface temperature anomalies. *J. Atmos. Sci.*, **42,** 1037–1049.

Held, I. M., and I. S. Kang, 1987: Barotropic models of the extratropical response to El Niño. *J. Atmos. Sci.*, **44,** 3576–3586.

——, S. W. Lyons and S. Nigam, 1989: Transients and the extratropical response to El Niño. *J. Atmos. Sci.*, **46,** 163–174.

Owen, J. A., and T. N. Palmer, 1987: The impact of El Niño on an ensemble of extended-range forecasts. *Mon. Wea. Rev.*, **115,** 2103–2117.

Randall, D. A., 1976: The interaction of the planetary layer with large-scale circulations. Ph.D. thesis, University of California, Los Angeles, 247 pp.

Rasmusson, E. M., and T. H. Carpenter, 1982: Variations in the tropical sea surface temperature and surface wind fields associated with the Southern Oscillation–El Niño. *Mon. Wea. Rev.*, **110,** 354–384.

Sardeshmukh, P. D., and B. J. Hoskins, 1988: Generation of global rotational flow by steady idealized tropical divergence. *J. Atmos. Sci.*, **45,** 1228–1251.

Shukla, J., 1981: Dynamical predictability of monthly means. *J. Atmos. Sci.*, **38,** 2547–2572.

——, and M. J. Fennessy, 1988: Prediction of time mean atmospheric circulation and rainfall: Influence of Pacific SST anomaly. *J. Atmos. Sci.*, **45,** 9–28.

Tokioka, T., K. Yamazaki and M. Chiba, 1987: A case study of the impact of sea surface temperature anomalies and initial conditions on dynamical forecast up to two months in the early summer of 1983. *Pap. Meteorol. Geophys.*, **38,** 265–277.

Trenberth, K. E., and J. G. Olson, 1988: An evaluation and intercomparison of global analyses from the National Meteorological Center and the European Centre for Medium Range Weather Forecasts. *Bull. Amer. Meteor. Soc.*, **69,** 1047–1056.

United States Navy, 1964: *World Atlas of Sea Surface Temperature.* Publication No. 225. Hydrographic Office.

Wallace, J. M., and D. S. Gutzler, 1981: Teleconnections in the geopotential height field during the Northern Hemisphere winter. *Mon. Wea. Rev.*, **109,** 784–812.

WMO, 1986: Workshop on comparison of simulations by numerical models of the sensitivity of the atmospheric circulation to sea surface temperature anomalies. WMO/TD-No. 138, WCP-121, 188 pp. [Available from World Meteorological Organization, Geneva.]